Uncertain but Useful: Leveraging CNN Variability into Data Augmentation

Inés Gonzalez-Pepe
Department of Computer Science
Concordia University
Montreal, QC H3G 1M8, Canada
inesgp99@gmail.com

Vinuyan Sivakolunthu
Department of Computer Science
Concordia University
Montreal, QC H3G 1M8, Canada
vinuyansivakolunthu@gmail.com

Yohan Chatelain
Krembil Centre for Neuroinformatics
Centre for Addiction and Mental Health
Toronto, ON M5T 0S8, Canada
yohan.chatelain@camh.com

Tristan Glatard
Krembil Centre for Neuroinformatics
Centre for Addiction and Mental Health
Toronto, ON M5T 0S8, Canada
tristan.glatard@camh.ca

Abstract

Deep learning (DL) is rapidly advancing neuroimaging by achieving state-of-the-art performance with reduced computation times. Yet the numerical stability of DL models—particularly during training—remains underexplored. While inference with DL is relatively stable, training introduces additional variability primarily through iterative stochastic optimization. We investigate this training-time variability using FastSurfer, a CNN-based whole-brain segmentation pipeline. Controlled perturbations are introduced via floating point perturbations and random seeds. We find that: (i) FastSurfer exhibits higher variability compared to that of a traditional neuroimaging pipeline, suggesting that DL inherits and is particularly susceptible to sources of instability present in its predecessors; (ii) ensembles generated with perturbations achieve performance similar to an unperturbed baseline; and (iii) variability effectively produces ensembles of numerical model families that can be repurposed for downstream applications. As a proof of concept, we demonstrate that numerical ensembles can be used as a data augmentation strategy for brain age regression. These findings position training-time variability not only as a reproducibility concern but also as a resource that can be harnessed to improve robustness and enable new applications in neuroimaging.

1 Introduction

Deep learning (DL) is increasingly adopted in neuroimaging, offering state-of-the-art performance and substantially reduced runtimes Henschel et al. [2022], Ren et al. [2025]. Despite their power, the numerical stability of DL models remains underexamined. Classical pipelines exhibit substantial variability from minor changes in preprocessing tools, software versions, or hardware Glatard et al. [2015], Chatelain et al. [2022], threatening reproducibility, particularly in studies with small sample sizes Peng [2011], Gorgolewski and Poldrack [2016]. This raises a key question: does DL overcome the numerical variability inherent in neuroimaging, or does it inherit similar instabilities?

Prior work suggests that DL inference is relatively stable Gonzalez Pepe et al. [2023, 2024], in contrast to the variability of traditional tools like FreeSurfer Fischl et al. [2002]. However, training introduces additional stochasticity through gradient-based optimization interacting with data shuffling, random seeds, and weight initialization. Unlike a single forward pass, training involves thousands of updates where small perturbations can accumulate. Yet, training-time variability in neuroimaging

39th Conference on Neural Information Processing Systems (NeurIPS 2025) Workshop: .

remains largely unexplored. Here, we investigate whether training convolutional neural networks (CNNs) introduces measurable variability, focusing on FastSurfer Henschel et al. [2022], a widely used CNN segmentation pipeline. We primarily inject numerical noise via Monte Carlo Arithmetic (MCA) Parker [1997], while also varying random seeds and weight initialization for comparison. Our study addresses two questions: (i) how does FastSurfer variability compare to traditional tools like FreeSurfer, and (ii) to what extent do models trained under different seeds, initialization schemes, or perturbations yield distinct yet valid solutions?

The resulting variability creates ensembles of model families, which can be exploited for new applications. For instance, while MCA-based augmentation has been proposed for diffusion MRI Kiar et al. [2021], our ensembles enable faster augmentation for various neuroimaging tasks. Our results reveal three key findings: (i) FastSurfer and FreeSurfer variability are comparable, showing that DL does not eliminate inherent neuroimaging variability; (ii) ensemble models achieve comparable performance while producing multiple distinct solutions; and (iii) numerical ensembles can serve as effective data augmentation, improving downstream tasks by leveraging the diversity of valid outputs.

2 Materials & Methods

FastSurfer Training Our study compares FastSurfer, a CNN-based whole-brain segmentation pipeline, with the classical FreeSurfer pipeline on a holdout subset of the CoRR data Zuo et al. [2014] used in prior work investigating inference variability Gonzalez Pepe et al. [2023]. FastSurfer was trained on FreeSurfer whole-brain segmentations, and, as in the original paper, all inputs to the model were preprocessed using FreeSurfer.

We mainly examine MCA, with variations in random seeds as a variability baseline and a fixed non-perturbed run as a default IEEE baseline. MCA is applied using the Fuzzy PyTorch tool Gonzalez-Pepe et al. [2025]. Fuzzy PyTorch introduces random perturbations to floating-point arithmetic at runtime that simulates rounding errors. Meanwhile, random seeds control the initial state of the pseudorandom number generators used during model training—for example, in shuffling data or initializing weights—ensuring reproducibility across runs. For this experiment, data shuffling was prevented and the data was fixed in order to keep the uncertainty epistemic and not aleatoric. Appendix A describes how to reproduce our FastSurfer experiments and Appendix B describes the Dice score, our main comparison metric, and details the sources of variability. Appendix C presents our MNIST sanity check, where we reproduced the FastSurfer experiment with MCA and random seed perturbations and initiated an analysis of variability from weight initialization.

FastSurfer Ensembling To illustrate the utility of numerical ensembling, we refer to previous work that leveraged MCA for data augmentation in diffusion MRI pipelines Kiar et al. [2021]. Similarly, outputs from different models in the FastSurfer ensembles (MCA, random seed) are all valid, indicating that FastSurfer's inherent variability can serve as an effective augmentation strategy. Introducing variability—incurs a one-time training cost. We focus on the random seed family, which trains fastest, and demonstrate its utility for brain age regression. Brain age prediction is a common neuroimaging task, as it can serve as a biomarker for neurodegenerative conditions. Using ROI volumes from FastSurfer training and test data as features in random forest and SVM regressors, each of 415 subjects had 10 FastSurfer repetitions, providing 10 distinct but valid ROI sets.

3 Results

We evaluate numerical stability across two axes: Monte Carlo Arithmetic induced numerical noise[1] and random seed perturbations.

CNN Models (FastSurfer) Are Susceptible to Numerical Variability Comparably To Traditional Neuroimaging (FreeSurfer). Figure 1 compares MCA and random seed–induced variability in FastSurfer training with MCA variability in FreeSurfer, using a CoRR data subset for ROIs in the left hemisphere.[2] Earlier work showed that FastSurfer was substantially less variable than FreeSurfer

[1]MCA training is ongoing due to its computational overhead and results are available only for the coronal model. For fairness, results in Figure 1 are reported at epoch 10. The Dice score at this point differs by 4%.

[2]We show only the left hemisphere for clarity, but the same trends hold in the right.

Figure 1: Variability comparison of minimum Dice scores across FastSurfer and FreeSurfer regions of interest (ROI). $\triangle$ indicate regions where FastSurfer is less variable, and $\triangledown$ where it is more variable than FreeSurfer (one-sided t-test, p<0.05, Bonferroni corrected). Subcortical ROIs are shown on the left, cortical on the right.

at inference for subcortical regions. For training, t-tests indicate that in 3 of 19 subcortical regions, FastSurfer is significantly less variable (denoted by $\triangle$). Overall, subcortical variability is largely comparable between FastSurfer and FreeSurfer.

In contrast, all cortical regions and 6 of 19 subcortical regions show statistically higher variability with FastSurfer (exploratory t-test results). Although MCA and random seed variability appear similar in magnitude, a two-sided t-test confirms they are distinct types of variability originating from different sources ($p = 4.45 \times 10^{-313}$). This higher cortical variability is unexpected and suggests areas for further investigation. Taken together, these results address our first research question: CNNs such as FastSurfer remain highly susceptible to numerical instability in whole-brain segmentation.

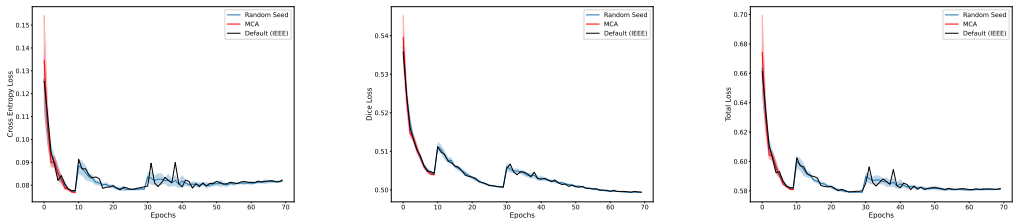

(a) Cross-Entropy Loss (b) Dice Loss (c) Weighted sum of all losses

Figure 2: Training loss variability across random seeds for FastSurfer coronal model. Axial, sagittal, and coronal models all exhibit the same pattern, so only the coronal is illustrated.

Models Within Ensembles Have Comparable Performance. We then investigate whether introducing variability during training affects overall model performance relative to a stable baseline. As a reference, we define the IEEE model, trained without MCA, with a fixed random seed, and a single initialization scheme. Figure 2 shows training loss trajectories, confirming that the numerical and random model families closely follow the IEEE baseline. We observe, large variability fluctuations mainly after the sharp drops in the learning curve caused by the cosineWarmRestarts learning rate schedule. Specifically, variability increases at restart epochs ($T_0 = 10$, $T_{multi} = 30$), reflecting inflection points where changes in learning rate amplify small differences between runs. For FastSurfer, across variability methods, models achieved performance comparable to the IEEE baseline.

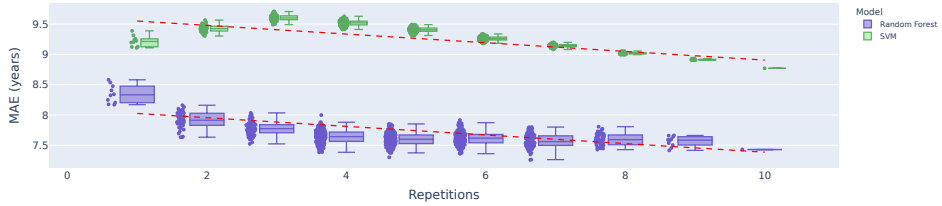

Figure 3: Linear regression illustrating the effect of data augmentation on performance mean absolute error (MAE) for FastSurfer data using Random Forest (Pearson's $R = -0.830$, $p = 2.932e-03$) and SVM (Pearson's $R = 0.803$, $p = 5.154e-03$) models.

Numerical Ensembling Serves as Data Augmentation Strategy. We observe random seed repetitions provide meaningful augmentation across models (Figure 3). Figure 3 shows that increasing repetitions consistently reduces test MAE, indicating that variability from the random seed family produces sufficiently diverse outputs to enhance predictive performance. This aligns with prior work suggesting that a few repetitions capture most of the benefit Lei et al. [2019], after which more sophisticated augmentation strategies may be preferable Cubuk et al. [2020], Li [2020]. Extreme MAE values in the first and last repetitions reflect smaller sample sizes. Using all 10 repetitions, the model achieves a test MAE of 7.40 years. The goal was not to achieve state-of-the-art performance (typically 2–5 years Leonardsen et al. [2022], Kumari and Sundarrajan [2024]) but to demonstrate the feasibility of numerical ensembles. Aggregating multiple FastSurfer repetitions provides a principled data augmentation strategy, yielding diverse yet valid outputs that improve predictive performance without additional data collection.

4 Conclusion

In this work, we systematically investigated the variability present in CNN training in neuroimaging, focusing on FastSurfer as a representative model. Our results demonstrate three key insights. First, FastSurfer and FreeSurfer exhibit comparable variability when examined under realistic perturbations, showing that DL models do not inherently eliminate numerical instability in neuroimaging pipelines. Second, families of models achieve performance comparable to a stable baseline, confirming that training-time stochasticity produces multiple high-performing yet distinct solutions without degrading overall model quality. Third, and most importantly, this inherent variability can be harnessed as a data augmentation strategy: repeated FastSurfer iterations provide diverse, valid outputs that improve downstream tasks, such as brain age regression, without additional data collection.

Taken together, these findings highlight that variability in CNN training contains useful signals. By systematically characterizing and leveraging this variability, researchers can enhance model robustness and predictive performance, bridging the gap between reproducibility concerns and practical utility in neuroimaging. More broadly, our study underscores the importance of understanding and exploiting training-time variability in DL models for scientific and clinical applications, and points to using ensembles for improving reliability and generalization.

References

PyTorch Implementation of FastSurferCNN. https://github.com/Deep-MI/FastSurfer. Accessed: 2024-09-28.

Yohan Chatelain, Nigel Yong Sao Young, Gregory Kiar, and Tristan Glatard. Pytracer: Automatically profiling numerical instabilities in python. *IEEE Transactions on Computers*, 72(6):1792–1803, 2022.

Ekin D Cubuk, Barret Zoph, Jonathon Shlens, and Quoc V Le. Randaugment: Practical automated data augmentation with a reduced search space. In *Proceedings of the IEEE/CVF conference on computer vision and pattern recognition workshops*, pages 702–703, 2020.

C. Denis, P. De Oliveira Castro, and E. Petit. Verificarlo: Checking Floating Point Accuracy through Monte Carlo Arithmetic. In *2016 IEEE 23nd Symposium on Computer Arithmetic (ARITH)*, pages 55–62, Los Alamitos, CA, USA, jul 2016. IEEE Computer Society. doi: 10.1109/ARITH.2016.31. URL `https://doi.ieeecomputersociety.org/10.1109/ARITH.2016.31`.

Bruce Fischl, David H Salat, Evelina Busa, Marilyn Albert, Megan Dieterich, Christian Haselgrove, Andre Van Der Kouwe, Ron Killiany, David Kennedy, Shuna Klaveness, et al. Whole brain segmentation: automated labeling of neuroanatomical structures in the human brain. *Neuron*, 33 (3):341–355, 2002.

Tristan Glatard, Lindsay B Lewis, Rafael Ferreira da Silva, Reza Adalat, Natacha Beck, Claude Lepage, Pierre Rioux, Marc-Etienne Rousseau, Tarek Sherif, Ewa Deelman, et al. Reproducibility of neuroimaging analyses across operating systems. *Frontiers in neuroinformatics*, 9:12, 2015.

Inés Gonzalez Pepe, Vinuyan Sivakolunthu, Hae Lang Park, Yohan Chatelain, and Tristan Glatard. Numerical Uncertainty of Convolutional Neural Networks Inference for Structural Brain MRI Analysis. In *International Workshop on Uncertainty for Safe Utilization of Machine Learning in Medical Imaging*, pages 64–73. Springer, 2023.

Inés Gonzalez Pepe, Yohan Chatelain, Gregory Kiar, and Tristan Glatard. Numerical stability of DeepGOPlus inference. *Plos one*, 19(1):e0296725, 2024.

Inés Gonzalez-Pepe, Hiba Akhaddar, Tristan Glatard, and Yohan Chatelain. Fuzzy pytorch: Rapid numerical variability evaluation for deep learning models. `https://github.com/big-data-lab-team/fuzzy-pytorch`, 2025. Accessed: 2025-09-03.

Krzysztof J Gorgolewski and Russell A Poldrack. A practical guide for improving transparency and reproducibility in neuroimaging research. *PLoS biology*, 14(7):e1002506, 2016.

Leonie Henschel, Sailesh Conjeti, Santiago Estrada, Kersten Diers, Bruce Fischl, and Martin Reuter. Fastsurfer-a fast and accurate deep learning based neuroimaging pipeline. *NeuroImage*, 219: 117012, 2020.

Leonie Henschel, David Kügler, and Martin Reuter. Fastsurfervinn: Building resolution-independence into deep learning segmentation methods—a solution for highres brain mri. *NeuroImage*, 251: 118933, 2022.

Gregory Kiar, Yohan Chatelain, Ali Salari, Alan C Evans, and Tristan Glatard. Data augmentation through monte carlo arithmetic leads to more generalizable classification in connectomics. *arXiv preprint arXiv:2109.09649*, 2021.

LK Soumya Kumari and R Sundarrajan. A review on brain age prediction models. *Brain Research*, 1823:148668, 2024.

Cheng Lei, Benlin Hu, Dong Wang, Shu Zhang, and Zhenyu Chen. A preliminary study on data augmentation of deep learning for image classification. In *Proceedings of the 11th Asia-pacific symposium on internetware*, pages 1–6, 2019.

Esten H Leonardsen, Han Peng, Tobias Kaufmann, Ingrid Agartz, Ole A Andreassen, Elisabeth Gulowsen Celius, Thomas Espeseth, Hanne F Harbo, Einar A Høgestøl, Ann-Marie De Lange, et al. Deep neural networks learn general and clinically relevant representations of the ageing brain. *NeuroImage*, 256:119210, 2022.

Sharon Y Li. Automating data augmentation: Practice, theory and new direction. *SAIL Blog*, 2020.

Ian B. Malone, David Cash, Gerard R. Ridgway, David G. MacManus, Sebastien Ourselin, Nick C. Fox, and Jonathan M. Schott. Miriad–public release of a multiple time point alzheimer's mr imaging dataset. *NeuroImage*, 70:33–36, 2013. doi: 10.1016/j.neuroimage.2012.12.044.

Daniel S. Marcus, Tracy H. Wang, Jill Parker, John G. Csernansky, John C. Morris, and Randy L. Buckner. Open access series of imaging studies (oasis): Cross-sectional mri data in young, middle aged, nondemented, and demented older adults. *Journal of Cognitive Neuroscience*, 19(9): 1498–1507, 2007. doi: 10.1162/jocn.2007.19.9.1498.

Daniel S. Marcus, Alexander F. Fotenos, John G. Csernansky, John C. Morris, and Randy L. Buckner. Open access series of imaging studies (oasis): Longitudinal mri data in nondemented and demented older adults. *Journal of Cognitive Neuroscience*, 22(12):2677–2684, 2009. doi: 10.1162/jocn.2009.21407.

Susanne G. Mueller, Michael W. Weiner, Leon J. Thal, Ronald C. Petersen, Clifford R. Jack, William Jagust, John Q. Trojanowski, Arthur W. Toga, and Laurel Beckett. Ways toward an early diagnosis in alzheimer's disease: the alzheimer's disease neuroimaging initiative (adni). *Alzheimer's & Dementia*, 1(1):55–66, 2005. doi: 10.1016/j.jalz.2005.06.003.

Douglass Stott Parker. *Monte Carlo Arithmetic: Exploiting Randomness in Floating-Point Arithmetic*. University of California (Los Angeles). Computer Science Department, 1997.

Roger D Peng. Reproducible research in computational science. *Science*, 334(6060):1226–1227, 2011.

Jianxun Ren, Ning An, Cong Lin, Youjia Zhang, Zhenyu Sun, Wei Zhang, Shiyi Li, Ning Guo, Weigang Cui, Qingyu Hu, et al. Deepprep: an accelerated, scalable and robust pipeline for neuroimaging preprocessing empowered by deep learning. *Nature Methods*, pages 1–4, 2025.

Ali Salari, Yohan Chatelain, Gregory Kiar, and Tristan Glatard. Accurate simulation of operating system updates in neuroimaging using monte-carlo arithmetic. In *Uncertainty for Safe Utilization of Machine Learning in Medical Imaging, and Perinatal Imaging, Placental and Preterm Image Analysis: 3rd International Workshop, UNSURE 2021, and 6th International Workshop, PIPPI 2021, Held in Conjunction with MICCAI 2021, Strasbourg, France, October 1, 2021, Proceedings 3*, pages 14–23. Springer, 2021.

David C. Van Essen, Stephen M. Smith, Deanna M. Barch, Timothy E.J. Behrens, Essa Yacoub, Kamil Ugurbil, and WU-Minn HCP Consortium. The wu-minn human connectome project: An overview. *NeuroImage*, 80:62–79, 2013. doi: 10.1016/j.neuroimage.2013.05.041.

Xi-Nian Zuo, Jeffrey S Anderson, Pierre Bellec, Rasmus M Birn, Bharat B Biswal, Janusch Blautzik, John Breitner, Randy L Buckner, Vince D Calhoun, F Xavier Castellanos, et al. An Open Science Resource for Establishing Reliability and Reproducibility in Functional Connectomics. *Scientific Data*, 1(1):1–13, 2014.

A Experimental Reproducibility

The code to reproduce this work is located at `https://github.com/InesGP/cnn_training_variability`.

A.1 Computational Infrastructure

The experiments were conducted on several clusters. Analysis was conducted on a server equipped with 8 compute nodes with 32 cores Intel(R) Xeon(R) Gold 6130 CPU @ 2.10GHz 22MB cache L3. Model training was conducted on

- the Nibi cluster hosted and operated by SHARCNET at University of Waterloo. of 134,400 CPU cores and 288 H100 NVIDIA GPUs
- the Speed cluster managed by the Concordia Gina Cody School of Engineering and Computer Science equipped with 24 32-core compute nodes, each with 512 GB of memory, 12 NVIDIA Tesla P6 GPUs, with 16 GB of GPU memory, 7 servers with 256 CPU cores each 4x A100 80 GB GPUs, partitioned into 4x 20GB MIGs each and 1 AMD FirePro S7150 GPU, with 8 GB of memory
- the Virya cluster managed by Concordia University equipped with 16 x V100 32GB Nvidia GPUs and 8 x A100 40GB Nvidia GPUs (presented as 16 x 20GB MIGs)

A.2 FastSurfer Training Methodology

A.2.1 FreeSurfer

FreeSurfer recon-all implements whole-brain segmentation Fischl et al. [2002], through a maximum a-posteriori estimation of the segmentation based on the non-linear registration of the subject image to an atlas by computing a maximum a posteriori (MAP) estimate of the segmentation W, given an input MRI scan I and the transform that registers the image into atlas space L, where the goal is to maximize $p(W|I, L)$;

$$p(W|I, L) \propto p(I|W, L)\, p(W)$$

$p(I|W, L)$ contains the probability for a given segmentation based off global spatial information and anatomical class statistics about image intensities obtained from the atlas space. $p(W)$ approximates the local spatial relationship between neighboring anatomical classes using anisotropic nonstationary Markov Random Fields. FreeSurfer is used to preprocess the data given to the FastSurfer model as well as to serve as a reference approach to the model, when both are evaluated on an unseen dataset (CoRR Zuo et al. [2014]). We use FreeSurfer v7.3.2, in order to match the version used by the FastSurfer authors during the original model training. To measure the variability in FreeSurfer whole brain segmentation, we applied MCA to FreeSurfer using “fuzzy libmath" Salari et al. [2021], a version of the GNU mathematical library instrumented with the Verificarlo Denis et al. [2016] compiler.

A.2.2 FastSurfer

FastSurfer [Henschel et al., 2022] is a CNN model that performs whole-brain segmentation, cortical surface reconstruction, fast spherical mapping, and cortical thickness analysis from anatomical MRIs. The FastSurfer CNN is composed of three 2D fully convolutional neural networks—each associated with a different 2D slice orientation—that each have the same encoder/decoder U-net architecture with skip connections, unpooling layers and dense connections as QuickNAT. A diagram of the model’s architecture is available in the Figure 4. We focus exclusively on the task of whole-brain segmentation, defined as voxel-wise anatomical labeling of brain regions. This segmentation step is entirely performed by the CNN, without surface reconstruction, and uses the pre-trained FastSurfer model (v2.4.0) available on GitHub [fas]. FastSurfer has demonstrated high accuracy, strong generalization to unseen datasets, and high test-retest reliability. This model serves as an ideal benchmark for studying numerical variability in high-dimensional medical imaging tasks due to its clinical relevance and architectural complexity.

We closely followed the methodology described in the original FastSurfer paper Henschel et al. [2022] and Github repository fas. We obtained access to all training and validation datasets used by the authors (HCP Van Essen et al. [2013], ABIDE-I, ABIDE-II, ADNI Mueller et al. [2005], IXI,

LA5C, MIRIAD Malone et al. [2013], OASIS1 Marcus et al. [2007], OASIS2 Marcus et al. [2009]), with the exception of the Rhineland Study dataset, due to data access restrictions, which we replaced with the MICA dataset, which has similar submillimeter resolution. All images were pre-processed using the FreeSurfer HiRes stream with the Desikan-Killiany-Tourville (DKT) atlas. The resulting segmentations were quality-controlled, and cases with failed segmentations were excluded. For model training, we used the configuration files provided for each anatomical plane, while introducing a perturbation effect across runs. In particular, to investigate the effect of weight initialization, we reinitialized the weights and biases of each layer according to the specific initialization scheme, while keeping all other hyperparameters fixed. Each model was trained for 70 epochs, and the best-performing checkpoint was kept for evaluation. Training typically takes about a day to a day and a half on GPU for the default and random seed models, while weight-initialization experiments can take up to 2.5 days. MCA experiments require over a month, as they must be run on CPU and involve a large computational overhead to perturb floating-point operations.

When comparing the FastSurfer model to the FreeSurfer baseline, we tested both methods on a subset of the Consortium for Reliability and Reproducibility (CoRR) dataset Zuo et al. [2014], as it aims to evaluate test-retest reliability and reproducibility and has previously been used for evaluating variability during FastSurfer inference Gonzalez Pepe et al. [2023]

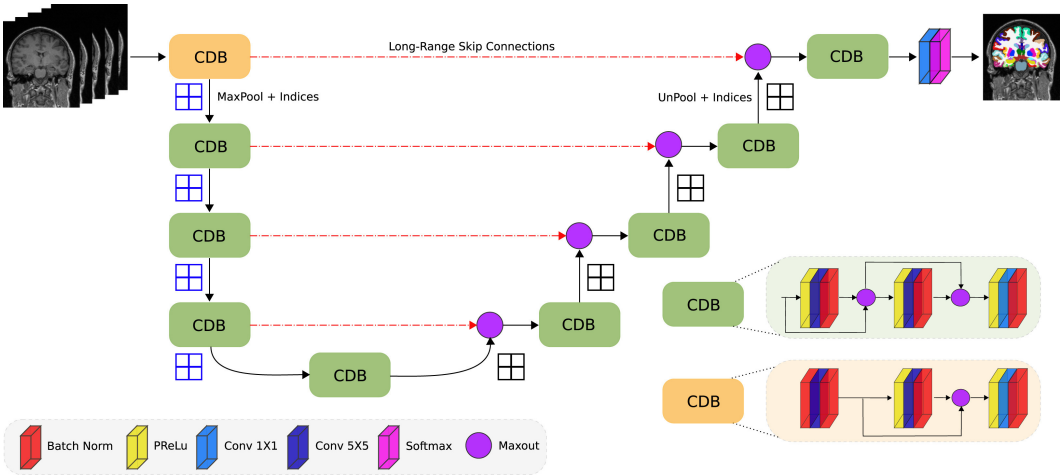

Figure 4: Illustration of FastSurfer's architecture. The CNN consists of four competitive dense blocks (CDB) in the encoder and decoder part, separated by a bottleneck layer. Figure reproduced from Henschel et al. [2020].

A.3 Data Use Acknowledgment

Data used in the preparation of this article were obtained from the Alzheimer's Disease Neuroimaging Initiative (ADNI) database (adni.loni.usc.edu). The ADNI was launched in 2003 as a public-private partnership, led by Principal Investigator Michael W. Weiner, MD. The original goal of ADNI was to test whether serial magnetic resonance imaging (MRI), positron emission tomography (PET), other biological markers, and clinical and neuropsychological assessment can be combined to measure the progression of mild cognitive impairment (MCI) and early Alzheimer's disease (AD). For up-to-date information, see adni.loni.usc.edu. Data collection and sharing for the Alzheimer's Disease Neuroimaging Initiative (ADNI) is funded by the National Institute on Aging (National Institutes of Health Grant U19AG024904). The grantee organization is the Northern California Institute for Research and Education. In the past, ADNI has also received funding from the National Institute of Biomedical Imaging and Bioengineering, the Canadian Institutes of Health Research, and private sector contributions through the Foundation for the National Institutes of Health (FNIH) including generous contributions from the following: AbbVie, Alzheimer's Association; Alzheimer's Drug Discovery Foundation; Araclon Biotech; BioClinica, Inc.; Biogen; BristolMyers Squibb Company; CereSpir, Inc.; Cogstate; Eisai Inc.; Elan Pharmaceuticals, Inc.; Eli Lilly and Company; EuroImmun; F. Hoffmann-La Roche Ltd and its affiliated company Genentech, Inc.; Fujirebio; GE Healthcare; IXICO Ltd.; Janssen Alzheimer Immunotherapy Research & Development, LLC.; Johnson & Johnson

Pharmaceutical Research & Development LLC.; Lumosity; Lundbeck; Merck & Co., Inc.; Meso Scale Diagnostics, LLC.; NeuroRx Research; Neurotrack Technologies; Novartis Pharmaceuticals Corporation; Pfizer Inc.; Piramal Imaging; Servier; Takeda Pharmaceutical Company; and Transition Therapeutics.

Data were provided [in part] by the Human Connectome Project, WU-Minn Consortium (Principal Investigators: David Van Essen and Kamil Ugurbil; 1U54MH091657) funded by the 16 NIH Institutes and Centers that support the NIH Blueprint for Neuroscience Research; and by the McDonnell Center for Systems Neuroscience at Washington University.

LA5C data was obtained from the OpenfMRI database. Its accession number is ds000030 Data were provided [in part] by OASIS-1: Cross-Sectional: Principal Investigators: D. Marcus, R, Buckner, J, Csernansky J. Morris; P50 AG05681, P01 AG03991, P01 AG026276, R01 AG021910, P20 MH071616, U24 RR021382, and OASIS-2: Longitudinal: Principal Investigators: D. Marcus, R, Buckner, J. Csernansky, J. Morris; P50 AG05681, P01 AG03991, P01 AG026276, R01 AG021910, P20 MH071616, U24 RR021382

Data used in the preparation of this article were obtained from the MIRIAD database. The MIRIAD investigators did not participate in analysis or writing of this report. The MIRIAD dataset is made available through the support of the UK Alzheimer's Society (Grant RF116). The original data collection was funded through an unrestricted educational grant from GlaxoSmithKline (Grant 6GKC).

ABIDE data was gathered from various dataset including the California Institute of Technologie funded by the Simons Foundation (SFARI-07-01 to R.A.) and the National Institute of Mental Health (R01 MH080721 to R.A.), the Carnegie Mellon University funded by NICHD/NIDCD PO1/U19 to M. B. (PI: Nancy Minshew), which is part of the NICHD/NIDCD Collaborative Programs for Excellence in Autism, and the Simons Foundation to M. B. (PI: David Heeger), the University of Leuven funded by the Flanders Fund for Scientific Research (FWO projects G.0758.10), the FWO postdoctoral Research fellowship grant (KA), the Grant P6/29 from the Interuniversity Attraction Poles program of the Belgian federal government, and the Leuven Autism Researc Consortium (LAuRes), funded by the Research Council of the University of Leuven (IDO/08/013), the Ludwig Maximilians University Munich, the NYU Langone Medical Center funded by NIH (K23MH087770; R21MH084126; R01MH081218; R01HD065282), Autism Speaks, The Stavros Niarchos Foundation, The Leon Levy Foundation, and an endowment provided by Phyllis Green and Randolph Cowen, the Olin, Institute of Living at Hartford Hospital, funded by Autism Speaks (to M.A.), and Hartford Hospital (to M.A) the Social Brain Lab BCN NIC UMC Groningen and Netherlands Institute for Neuroscience funded by Nederlandse Organisatie voor Wetenschappelijk Onderzoek (NWO) Cognitive Pilot Project (051.07.003), NWO VIDI (452-04-305), the NWO Open Competition (400-08-089), the European Commission, Marie Curie Excellence Grant (MEXT-CT-2005-023253), the National Initiative for Brain and Cognition NIHC HCMI Functional Markers (056-13-014), the National Initiative for Brain and Cognition NIHC HCMI Simulation and TOM (056-13-017), and the Netherlands Brain Foundation (KS 2010(1)-29) the Trinity Centre for Health Sciences funded by The Meath Foundation, Adelaide and Meath Hospital, incorporating the National Children's Hospital (AMNCH), Tallaght, and travel fellowship by the Kyulan Family Foundation. the University of Michigan funded by Autism Speaks (CSM), NIH U19 HD035482 and NIH MH066496 (CL), Autism Speaks Pre-doctoral Fellowship 4773 (JLW), the Michigan Institute for Clinical and Health Research (MICHR) Pre-doctoral Fellowship UL1RR024986 (JLW), and NIH R21 MH079871 (SP) the Indiana University funded by National Institutes of Health Grant K99MH094409/R00MH094409 (to D.P.K.) the Erasmus University Medical Center Rotterdam funded by the Simons Foundation Autism Research Initiative (SFARI -307280) and a Dutch ZonMw TOP grant number 91211021 to Tonya White. MRI data acquisition was sponsored in part by the European Community's 7th Framework Programme (FP7/2008-2013 212652). Supercomputing computations were supported by the NWO Physical Sciences Division (Exacte Wetenschappen) and SURFsara (Lisa compute cluster, www.surfsara.nl). The Generation R Study is conducted by the Erasmus Medical Center in close collaboration with the School of Law and Faculty o Social Sciences of the Erasmus University Rotterdam, the Municipal Health Service Rotterdam area, Rotterdam, the Rotterdam Homecare Foundation, Rotterdam and the Stichting Trombosedienst & Artsenlaboratorium Rijnmond (STAR-MDC), Rotterdam.

The IXI data was obtained from their website at https://brain-development.org/ixi-dataset/

B Methods Supplementary

B.1 Model Perturbations

Fuzzy PyTorch To simulate numerical perturbations during training, we employ MCA using the Fuzzy PyTorch tool Gonzalez-Pepe et al. [2025]. Fuzzy PyTorch introduces random perturbations to floating-point arithmetic at runtime that simulates rounding errors by applying the following perturbation to all floating-point operations of an application:

$$random\_rounding(x \circ y) = round(inexact(x \circ y))$$

where x and y are floating-point numbers, $\circ$ is an arithmetic operation, and $inexact$ is a random perturbation defined at a given virtual precision:

$$inexact(x) = x + 2^{e_x - t}\xi$$

where e_x is the exponent in the floating-point representation of x, t is the virtual precision, and $\xi \sim U(-\frac{1}{2}, \frac{1}{2})$ is a uniform random variable.

Random Seeds In PyTorch, random seeds control the initial state of the pseudorandom number generators used during model training—for example, in shuffling data or initializing weights—ensuring reproducibility across runs. For this experiment, data shuffling was prevented and the data was fixed in order to keep the measured uncertainty epistemic and not aleatoric. For the random seed experiment, we train models using 10 different random seeds (0–9), which affect dropout, and initial weight sampling. This enables us to isolate the effects of deterministic initial states from stochastic numerical variation.

Weight Initializations Weight initialization refers to the strategy used to set the initial values of the model's parameters before training begins. These initializations can significantly impact model convergence and performance. For the weight initialization experiment, we assess the following initialization strategies implemented in PyTorch, including `dirac`, `identity`, `kaiming_normal`, `kaiming_uniform`, `orthogonal`, `sparse`, `xavier_uniform`, and `xavier_normal`. Note, in Appendix C, during the MNIST sanity check, `uniform`, `normal`, `zeros`, and `ones` were excluded from analysis due to severe degradation in accuracy and outlier behavior.

B.2 Sørensen-Dice Scores

To assess the impact of variability on segmentations, we compute the minimum Sørensen-Dice score across pairs of repetitions. The Sørensen-Dice score measures the overlap between two segmentation results and is commonly used to quantify similarity between labeled regions in medical imaging. Given N different segmentations, each segmentation output assigns a class label to every voxel in the MRI. Let S_i and S_j represent the set of voxels assigned to a specific brain region in the i-th and j-th iterations, respectively. The Sørensen-Dice score for these two sets is given by:

$$\text{min Sørensen-Dice Score} = \min_{\substack{i,j \in \{1,\ldots,N\} \\ i \neq j}} \left(\frac{2 \cdot |S_i \cap S_j|}{|S_i| + |S_j|} \right)$$

where $|S_i \cap S_j|$ is the number of overlapping voxels classified as part of the same region in both segmentations, and $|S_i| + |S_j|$ are the total number of voxels assigned to that region in each iteration. Taking the minimum across all pairs highlights the worst-case consistency between segmentations, making it a conservative measure of variability.

In practice, when the Dice score is used as a loss function during training, it is formulated as the Dice loss, defined as 1 minus a probabilistic Dice coefficient computed between the normalized predicted probability map and the ground-truth labels.

C MNIST Benchmark

To generalize beyond FastSurfer, we repeated these experiments on a CNN trained on MNIST. Here, weight initialization again dominated variability, with differences on the order of 10^{-1} in validation loss (Figure 5). MCA and random seed perturbations remained comparatively minor ($\sim 10^{-3}$), though random seeds produced larger deviations ($\sim 10^{-2}$) early in training—consistent with their influence on initialization and dropout. Figure 6 highlights the performance impact: while

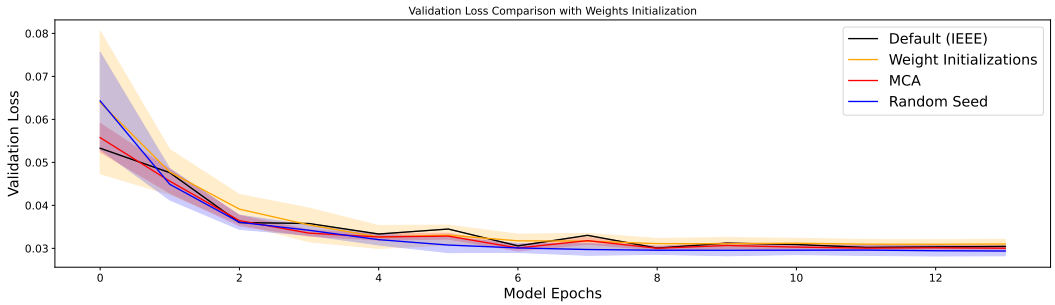

Figure 5: Comparison of sources of variability across validation loss for MNIST model

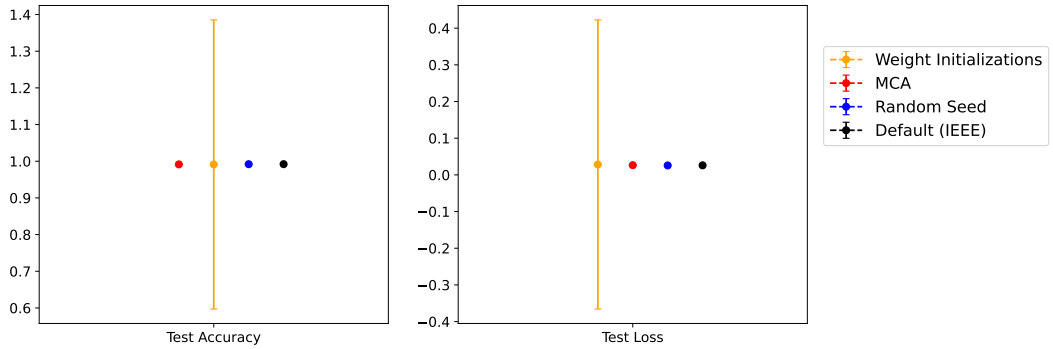

Figure 6: Comparison of sources of variability across test accuracy and loss for MNIST model

weight initialization reduced test accuracy to as low as 94%, both MCA and random seed variability maintained near-baseline accuracy ($\sim 99\%$).